Journal of Bioremediation & Biodegradation

Idrees, et al., J Bioremediat Biodegrad 2018, 9:1
DOI: 10.4172/2155-6199.1000421

Research Article Open Access

Carbonic Anhydrase II Based Biosensing of Carbon Dioxide at High Temperature: An Analytical and MD Simulation Study

Danish Idrees[1*], Razique Anwer[2], Mohd Shahbaaz[3], Myalowenkosi Sabela[4], Khalid I Al Qumaizi[5], Osama A Al Khamees[6], Samudrala Gourinath[1], Manoj Kumar[7] and MP Singh[7]

[1]*School of Life Sciences, Jawaharlal Nehru University, Delhi, India*

[2]*Department of Anatomy (Microbiology), College of Medicine, Al Imam Mohammad Ibn Saud Islamic University (IMSIU), Riyadh, Saudi Arabia*

[3]*South African National Bioinformatics Institute, University of the Western Cape, Private BagX17, Bellville, Cape Town, South Africa*

[4]*Department of Chemistry, Durban University of Technology, Durban 4000, South Africa*

[5]*Department of Family Medicine, College of Medicine, Al Imam Mohammad Ibn Saud Islamic University (IMSIU), Riyadh, Saudi Arabia*

[6]*Department of Pharmacology, College of Medicine, Al Imam Mohammad Ibn Saud Islamic University (IMSIU), Riyadh, Saudi Arabia*

[7]*Indian Oil Corp Ltd, Research and Development Centre, Faridabad, India*

[*]**Corresponding author:** Danish Idrees, School of Life Sciences, Jawaharlal Nehru University, Delhi, India, Tel: 9911651302; E-mail: danish.idress@gmail.com

Rec date: November 14, 2017; **Acc date:** November 23, 2017; **Pub date:** November 27, 2017

Copyright: © 2017 Idrees D, et al. This is an open-access article distributed under the terms of the Creative Commons Attribution License, which permits unrestricted use, distribution, and reproduction in any medium, provided the original author and source are credited.

Abstract

Concentration of carbon dioxide (CO_2) in the atmosphere has increased significantly due to anthropogenic activities and attributed as a major factor to global warming. Its detection by biosensing methods will provide an alternative for the assessment of CO_2 concentration. Biomineralization of CO_2 is one of the available methods for the biological conversion of CO_2 to carbonate using a highly active enzyme, carbonic anhydrase II (CAII). CAII was used for the carbonation reaction to convert CO_2 to $CaCO_3$. The precipitation of calcium carbonate ($CaCO_3$) was promoted in the presence of the CAII at 325 K. CAII showed an enhanced formation of solid $CaCO_3$ through the acceleration of CO_2 hydration rate at 325 K. Furthermore, the electrocatalytic properties of glassy carbon electrode enable us to determine the reduction peak potential values of CO_2 through cyclic voltammetry at –1.75 and 0.3 V at 325 K. Molecular dynamic (MD) simulations were performed each at 50 ns time scale provided a deeper insight into the molecular basis of the CAII interaction with CO_2 at different temperatures, highlighted that the CAII can detect CO_2 up to 325 K. We assume that CAII could be an effective and economical biosensor for biomineralization of CO_2 at high temperature 325 K.

Keywords: Carbon dioxide sequestration; Calcium carbonate; Biomineralization; MD simulations; Carbonic anhydrase II

Introduction

Carbon dioxide (CO_2), gas is considered as one of the main atmospheric components responsible for a greenhouse effect and also responsible for the increase of atmospheric temperature [1,2]. Hence, it is demand for increasing environmental awareness to find a solution for CO_2 mitigation [3]. The capture of anthropic CO_2 released in the atmosphere by human activities is one of the challenging problems worldwide [4]. Two significant approaches are used to reduce the concentration of CO_2 in the atmosphere, in which CO_2 can either recovered from industrial flue gases and transport it to suitable locations for storage or CO_2 can be sequestered using chemical fixation method to get carbomate minerals, such as calcite, magnesite, and dolomite [5,6]. The conversion of CO_2 into solid carbonates offers a possibility of a safe and stable ecofriendly product for long term carbon sequestration. Moreover, mineral based sequestration produces useful products such calcium carbonate ($CaCO_3$) or magnesium carbonate ($MgCO_3$), which are solid and can easily be precipitated [7]. The hydration of CO_2 to form carbonic acid is the slowest and rate-limiting step [8]. The conversion of CO_2 into carbonate ions was found to be a forward reaction with a rate constant of 6.2×10^{-3} s at 25°C [9]. A biological catalyst, carbonic anhydrase (CA) has been used to increase the rate of hydration of CO_2, to overcome the rate-limiting step, a biological catalyst.

Carbonic anhydrase (CA, EC 4.2.1.1) is a metallo-enzyme, present in both prokaryotes and eukaryotes and perform varieties of functions such as pH homeostasis, renal acidification, gluconeogenesis, bone resorption, respiration and ion transport [10,11]. CA catalyzes the reversible hydration and dehydration of CO_2 and bicarbonate, respectively. CA has the high affinity for CO_2 and easy to capture the atmospheric. Human CAII is highly active and has a kcat/KM of 1.5×10^8 Ms^{-1} [12,13] with highest turnover number (kcat 10^6 s^{-1}).

Thus, CAII is a suitable candidate for sequestration of CO_2 because of its increasing industrial interest. CAII has already been reported as a bio-catalyst for carbon sequestration of the flue gas from coal-fired power plants [14]. In addition, there is also interest in exploiting CA in algae as a way to capture CO_2 and convert it into biofuels or other valuable products [15,16]. Furthermore, CO_2 hydration can be significantly enhanced (10^7 times) by CA [17,18]. However, use of the free enzyme in solution has also many serious drawbacks, such as low stability that limits re-usability, recovery and cost in an industrial setting [19].

In the present work, MD simulations of CAII at different temperature ranges were performed to investigate the stability of CAII against temperature. The molecular mechanism of CO_2 detection at three different temperatures (300 K, 310 K and 325 K) was understood

on the basis of the outcome obtained from MD simulations, in which behavior was analyzed at three different temperatures for 50 ns time scale. To validate the outcome of MD simulations, CAII was sub-cloned cDNA of human CAII in the expression vector pET15d. Open reading frame (ORF) for CAII is of 801 base pairs encoded 267-amino acids. We constructed vector including the sequence coding for a CAII protein and an N-terminal poly-histidine (6XHis) tag to simplify the detection of protein expression using antibodies specific for the tag. Purification of recombinant protein was performed using immobilized metal affinity chromatography followed by gel filtration. The purified protein was used for precipitation of CO_2 (aq) into $CaCO_3$ in the presence of calcium ions at high temperature (325 K). Furthermore, the CAII based detection of the CO_2 at 325 K was analyzed by using the electrochemical methods.

Materials and Methods

Materials

E. coli strains DH5α (Invitrogen, California, USA) and Origami BL21 (DE3) (Novagen, Wisconsin, USA) were used for cloning and expression of recombinant protein, respectively. The *E. coli* cells harboring recombinant plasmids were grown aerobically in Luria-Bertani (Merck, Darmstadt, Germany) broth with 100 µg/µl Ampicillin (Sigma, Saint Louis, MO, USA). Plasmid pET15d (Novagen, Wisconsin, USA) was used as an expression vector. Plasmid isolation, restriction enzyme digestion, ligation, and competent cell preparation were carried out by standard procedures.

Molecular dynamic simulations

The structure of CAII was modelled by using the MODELLER module of the Discovery Studio 2016 (DS, http://accelrys.com/products/collaborative-science/biovia-discovery-studio/). The modelled structure of CAII was minimized by using the CHARMM force field [20] based optimization modules of DS. Similarly, the structure of CO_2 was constructed by utilizing the drawing utilities present in the DS and structure was optimized by using the DFT method implemented in the Dmol3 module of the DS.

Furthermore, the molecular docking was performed by using the CDOCKER module which is a CHARMM [20] force field based docking algorithm implemented in DS. The understanding about the active site of the CAII was obtained from the literature [21]. The CO_2 was docked in the active site of CAII and around 10 conformations generated for the further study. The generated conformations were re-scored, and best docked pose was selected for the MD simulation studies.

The selected docked structures of CAII and CO_2 were subjected to MD simulations using GROMACS [22] (version 5.1.2, installed on the Center for High Performance Computing (CHPC), Cape Town which provide 10 nodes with 24 cores per node of space for computation). The topology of CAII was produced on the basis of GROMOS96 53a6 force field [23]. Due to the unavailability of suitable force field parameters for drug-like molecules in the GROMACS package, the PRODRG server [24] was used for the generation of the CO_2 topologies and coordinate files. The partial charges were corrected by using DFT method of Gaussian which utilized the B3LYP 6-31G (d,p) basis set and CHELPG program [25]. After the successful topology generation, the docked complex was immersed in SPC/E water model [26] and the system was neutralized by adding the counter ions. The neutralized system was energetically minimized by utilizing the steepest descent and conjugate gradient algorithms with a convergence criterion of 0.005 kcal mol^{-1}. In order to increase the reliability of the MD simulations the restrains were applied to the structure of the piperine before the equilibration phase.

The equilibration phase was carried out separately in NVT (constant volume) as well as NPT (constant pressure) ensemble conditions, each for 100 ps time scale. The temperature of the system was changed from 300 K-325 K in both ensemble conditions along with pressure which was maintained at 1 bar by utilizing Parrinello-Rahman barostat in constant pressure ensemble. The final MD simulations were produced on the basis of LINCS algorithm at 50 ns time scale. The knowledge extracted from the trajectory files were utilized for the analyses of each complex behavior in the explicit water environment. The distances, H-bonds and RMSD (Root Mean Square Deviations) and several other parameters were analyzed for CAII – CO_2 complex.

Cloning and expression of CAII

The CAII gene was subcloned into pET15d vector (Novagen, EMD Biosciences, Madison, Wisconsin, USA) and cloning was confirmed through colony PCR and restriction digestion. The expression vector, pET15d, containing the full-length coding region of CAII gene was transformed into *E. coli* BL21(DE3) host cells by following the standard molecular biology protocol. The overnight culture of the expression cells from a freshly transformed plate was inoculated in LB media, containing 100 µg/µl ampicillin, and incubated, with constant agitation at 220 rpm in an incubator shaker until the absorbance was 0.6 at 600 nm. The culture was induced by 0.25 mM IPTG, and incubated for 4 hours with constant shaking. The cells were harvested, resuspended and sonicated. Cell extract after sonication was centrifuged at 12000 g for 30 min, and the pellets were discarded while supernatant was collected for the purification.

Protein purification

The filtered supernatant was loaded on previously equilibrated Ni-NTA column, with 5 column volumes (CV) of equilibration buffer. Elution was performed with increasing concentration of imidazole. Fractions were analyzed by sodium dodecyl sulphate-polyacrylamide gel electrophoresis (SDS-PAGE). Fractions containing CAII were pooled together, concentrated and loaded on the size exclusion column, HiPrep Superdex 75 (GE Healthcare Bio-Sciences), equilibrated with 150 ml of buffer and run at 0.5 ml/min. The chromatogram was monitored using Unicorn software (GE Healthcare Bio-Sciences). Fractions containing pure CAII were used for further analysis. The purity of purified protein was checked by SDS-PAGE. Furthermore, purified CAII was confirmed by Western blot.

Determination of CAII activity

The CAII activity was measured according to Sharma et al. [27]. In brief, CO_2 saturated water prepared by introducing CO_2 in 500 ml of Milli Q pure water for 1 h at 325 K. CO_2 saturated water (3 ml) was immediately added to 2 ml of Tris-HCl buffer (100 mM; pH 8.3), and 0.1 ml of free purified CA (1 mg/ml stock). The time required for the pH change 8.0–7.0 (t) was measured using Beetrode electrode with separate reference electrode (Dri-Ref), manufactured by World Precision Instruments Incorporation (WPI). The time required for the pH change (8.0-7.0) was used as control (tc), when buffer was

substituted for test sample. The enzyme assay was carried out at 325 K. The Wilbur Anderson units were calculated with the equation (tc–t)/t. The measurements were carried out in three replicates.

Enzymatic carbon dioxide capture

The CA purified was used as a catalyst in the capture of CO_2 by precipitation in the form of $CaCO_3$ at high temperature (325 K). The reaction mixture consists of 7.5 mL of the purified enzymatic extract, 7.5 mL of 1.2 M Tris-HCl buffer pH 10.5 solution containing 4.5% (w/v) $CaCl_2$ and 30 mL of the CO_2 solution. The CO_2 solution was prepared by bubbling deionized water with gaseous CO_2 at 325 K. The reaction started when the CO_2 solution was added into the flask that was immediately closed with a sealing film. In all experiments the temperature was maintained at 325 K. The mixture was then filtered and dried after 8 and 120 min of reaction to determine the weight of $CaCO_3$ precipitated (enzymatic assay). At the same time samples were prepared by replacing the enzyme with deionized water (non-enzymatic assay) and the results expressed as the difference between the values obtained in the enzymatic assay and those obtained in the non-enzymatic assay ($\Delta CaCO_3$), calculated according to Eq. (1). For use in CO_2 capture, the enzyme purified by ammonium sulfate precipitation was dialyzed to remove the salt. The reaction was performed at 325 K. $CaCO_3$ ¼ m $CaCO_3$ EA _ m $CaCO_3$ NEA ð1Þ where m $CaCO_3$ EA is the weight of $CaCO_3$ in the enzymatic assay (g) and m $CaCO_3$ NEA is the weight of $CaCO_3$ in the non-enzymatic assay (g).

XRD and WDXRF analysis

XRD pattern of powdered samples were recorded with X-ray diffractometer (Rigaku D-max 2500 PC, Japan) in the 2θ range of 3 to 75° at a scanning speed of 2 deg/min and a step size of 0.01°. The XRD pattern was processed and presence of various crystalline phases in the sample was determined by search match software. To confirm the presence of the phases identified by XRD, elemental analysis was carried by WDXRF. Crystallite size of the crystalline phases was obtained from FWHM of the XRD peaks. Elemental analysis of the sample was carried out by WDXRF (Axios, PANalytical, Netherlands). The sample was packed in the sample cell and then analyzed by WDXRF using standard-less semi-quant software. XRF spectra were processed and presence of various elements was identified using the software. Semi-quantitative results were obtained from standard-less semi-quant software.

TEM analysis

TEM experiments were performed on a JEOL JEM 2100 TEM (200 kV accelerating voltage). The powdered samples were dispersed in ethanol solvent by ultrasonication and the resulting suspension was deposited onto 200 mesh Cu grids covered with formvar and a holey carbon support film. Particle size and shape were obtained from the TEM image.

Electrochemical measurements

The electrochemical behavior of CO_2 was studied using a three-electrode system (working electrode: glassy carbon electrode; auxiliary electrode: platinum wire; reference electrode: SCE). Prior to analysis of the analyte, the glassy carbon electrode was polished using 0.5 µm alumina powder followed by electrochemical cycles in 0.5M H_2SO_4 solution till a stable voltammetric response was achieved.

To ensure that there was continuous flow of CO_2 into the polarographic cell, the VA computrace setup was modified accordingly by connecting an addition gas tube that delivered CO_2 directly into the measuring solution. The CO_2 gas was produced from the reaction of 0.5 g Na_2CO_3 with 6 M HCl. The 18 ml of HCl was allowed to react drop by drop (18 ml/25 s) in a closed system allowed for consistent flow of CO_2 into the measuring cell in which the three-electrode system was immersed. Cyclic Voltammetry measurements were performed from -2 to 2 V and 0 to 0.8 V at high temperature. Differential Pulse Voltammery (DPV) was performed from -2.0 to 0 V. All electrochemical measurements were performed at 100 mV. S^{-1} and deposition time of 40 s following the two approaches: (a) buffer, CAII and CO_2; (b) buffer, saturation with CO_2 and CAII.

Results

Molecular dynamic simulations

MD simulations provide a dynamic picture of CAII and CO_2 complex. MD simulations were performed at different temperature each for 50 ns and their trajectories were analyzed by using the utilities of the GROMACS. The distance between the CAII and CO_2 of the complex were remaining relatively similar at all different temperature (Figure 1). Dynamic stability of CAII and CO_2 complex, over the simulation of 50 ns was analyzed using backbone RMSD of Cα atoms. RMSD result showed a varied nature. At 300 K, the RMSD values were fluctuating and the magnitude of the values decreases. The similar fluctuating behavior was observed for CAII and CO_2 complex at 310 K and 325 K with the RMSD values increases (Figure 2A). Furthermore, the Rg analysis was performed to measure the compactness of CAII and CO_2 complex. The average value of Rg, calculated from trajectory showed similar behavior for all different temperatures, relatively larger fluctuations were observed at 325 K (Figure 2B). The RMSF was also calculated at all different temperature and found to consistent with RMSD and Rg. The RMSF values showed higher fluctuation at 325 K as compared to the other conditions (Figure 2C).

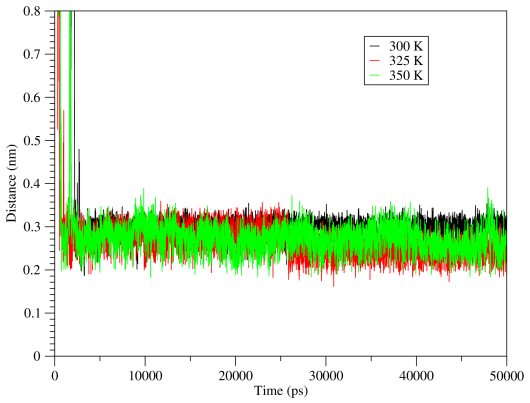

Figure 1: The graphical representation of the fluctuation observed in the distance between CAII and CO_2 during the course of each 50 ns MD at different temperature.

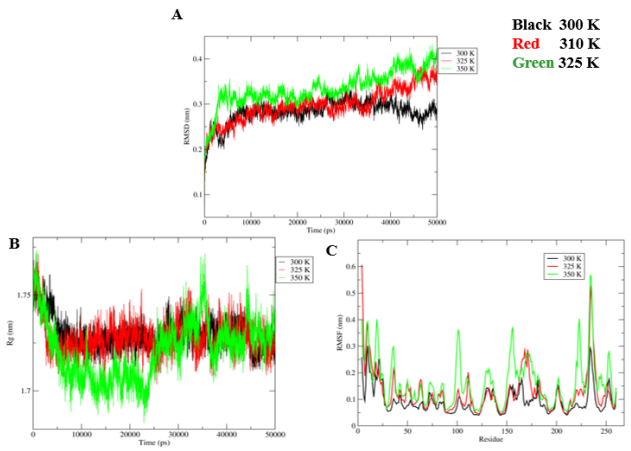

Figure 2: The graphical representation of the variations in (A) RMSD values at different temperature (B) Rg values at diverse temperature (C) RMSF values.

Expression and purification of CAII

CAII was cloned in pET15d, and then constructed plasmid was verified by DNA sequencing. This constructed plasmid pET15d-CAII was transformed into *E. coli* BL21 (DE3) strain, and induced with 0.25 mM IPTG accumulates high amounts of a soluble protein migrating in SDS-PAGE with an apparent molecular weight of 29 kDa. SDS PAGE analysis also showed that CAII was expressed as a monomer and CAII was found in the soluble bacterial extract (supernanat).

CAII purified from the Ni-NTA affinity showed contamination by other proteins (Figure 3A). We used gel filtration chromatography to further purify the CAII. We found that CAII was eluted at 70 ml of elution volume which is an indication that the existence of monomer form (Figure 3B). The purity of gel filtration eluent was further confirmed using SDS-PAGE that clearly showing a single band (Figure 3C).

S. No.	Mass Mr.	Range	P sequence
1	934.4509	81-89	GGPLDGTYR
2	1168.515	172-181	SADFTNFDPR
3	1580.81	114-126	YAAELHLVHWNTK
4	1667.961	133-148	AVQQPDGLAVLGIFLK
5	2139.085	40-58	YDPSLKPLSVSYDQATSLR
6	2248.107	114-132	YAAELHLVHWNTKYGDFGK
7	2248.1065-83	114-132	YAAELHLVHWNTKYGDFGK
8	2335.258	127-148	YGDFGKAVQQPDGLAVLGIFLK
9	2473.224	59-80	ILNNGHAFNVEFDDSQDKAVLK
10	2633.527	133-158	AVQQPDGLAVLGIFLKVGSAKPGLQK

Table 1: List of peptide fragments obtained after trypsinization.

The total amount of CAII being purified from a 20 g pellet is 60 mg. Recombinant CAII protein was confirmed by Western blot that showing a molecular weight of about 29 kDa (Figure 3D). CAII was further confirmed by MALDI-TOF and its peptide mass fingerprint. The CAII was confirmed by peptide sequences shown in Table 1 which were used for homology search.

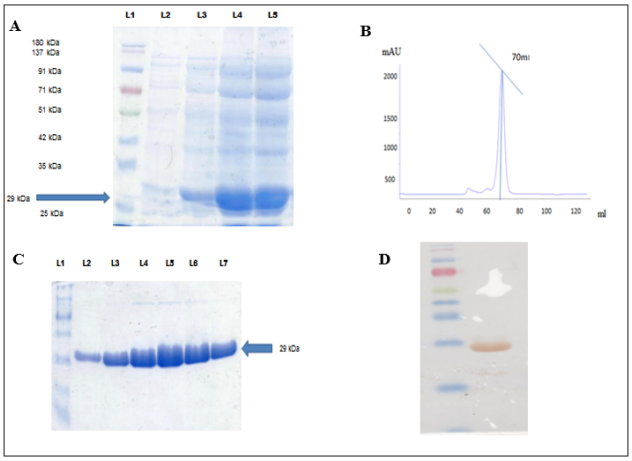

Figure 3: Purification of CAII (A). SDS-PAGE analysis of recombinant CAII with stained with coomassie brilliant blue. Lane1 is marker, Lane 2 is flow through, Lane 3 is washing and Lane 4 and 5 are CAII purified by Ni-NTA affinity chromatography. (B). Gel filtration elution profile of CAII loaded on HiLoad 16/600 Superdex 75 (GE Healthcare Life Sciences). (C). SDS-PAGE of purified CAII. (D) Western blot showing human CAII with anti-His– HRP conjugate.

Hydration of carbon dioxide with and without CAII

CA catalyzes the hydration of CO_2, and consequently hydrogen ions are transferred between the active site of the enzyme and the surrounding buffer. These results in the decrease of pH at a formation of HCO_3^- rate so fast that the over-all precipitation of $CaCO_3$ rate may itself decrease.

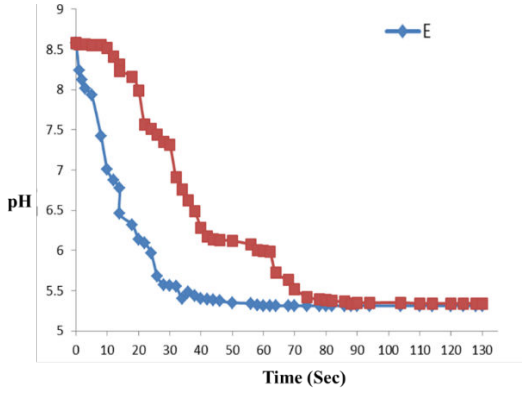

Figure 4: Enzymatic hydration of CO2 using the enzyme CAII at high temperature.

Therefore, measuring the pH is a viable method to monitor the progress of this enzymatic reaction at high temperature 325 K. Figure 4 shows the decrease in pH during the assay for CA using the enzyme obtained. The curves show that this enzyme was a very effective catalyst for hydration of CO_2.

Acceleration of carbonate formation by CA

As shown in Table 2, the amounts of calcium carbonate precipitated after 15, 30, and 60 sec is significantly higher than the control without enzyme at high temperature. CAII accelerates the formation of bicarbonate ions by lowering the activation energy required for hydration of CO_2. The conversion of CO_2 into H_2CO_3 is the rate controlling step catalyzed by CAII, while the formation of HCO_3^- is nearly diffusion controlled [28]. However, the conversion of HCO_3^- to CO_3^{2-} is pH dependent. An enzyme can only increase the rate of the reaction, but could not alter it, thus CA is deemed to accelerate the formation of bicarbonate ions. Under the precipitation conditions (pH 9.0–9.5) bicarbonate ions exist in equilibrium with carbonate ions and in presence of calcium ions result in calcium carbonate precipitation. Thus, CA plays the important role in hydration reaction corresponding to calcium carbonate formation; hence the in presence of enzyme the higher amount of the $CaCO_3$ is obtained.

Time (Sec)	$\Delta CaCO_3$ (g)
15	0.0108+0.0008
30	0.0324+0.0010
60	0.1017+0.0021

Table 2: Results obtained in the enzymatic precipitation of carbon dioxide.

The effect of the concentration of enzyme on the time to onset the start of precipitation and amount of the precipitation was also studied (data not shown). We found to direct relation between the concentration of enzyme with time taken to onset of precipitation and amount of precipitation. Ores et al. and Byung also demonstrated that the total mass of $CaCO_3$(s) precipitated do not depend on the concentration of the enzyme which, as a catalyst, can only change the kinetics to reach equilibrium that occurs in the first minutes of reaction, not the equilibrium thermodynamics [29-31].

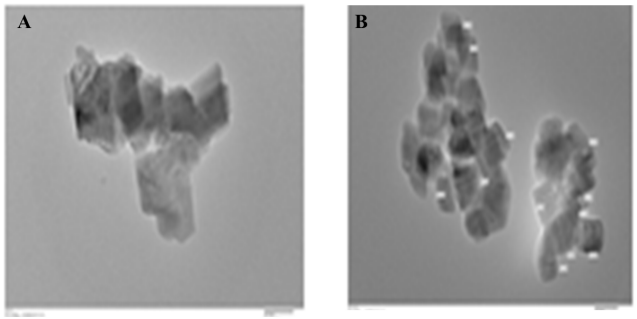

Figure 5: TEM image of $CaCO_3$ produced (A) with CAII and (B) without CAII at high temperature.

The XRD spectra of calcium carbonate ($CaCO_3$) which has three crystal phases (calcite, aragonite, and vaterite). Among three the calcite phase is a thermodynamically most stable phase under the ambient conditions (Figure 5).

The TEM analysis showed that in the presence of enzyme CAII nano particle of $CaCO_3$ was found irregular in size from 60 to 150 nm in presence of enzyme while without enzyme the size was not irregular in shape with size around 500 nm as shown in Figures 5A and 5B.

Electrochemical measurements

Electrochemical measurements demonstrated three significant observations within the potential range -2.0 to 0.1 V. The observable peaks were further explored in a narrow potential range namely: -2.0 to 0.0 V; -1.4 to -0.6 and lastly at 0.0 to 0.8 V (vs Ag/AgCl). The two approaches used complemented one another in a sense that they confirmed that CAII participate in the detection of CO_2. The obtained peaks in the electrochemical detection were illustrated in Figure 6.

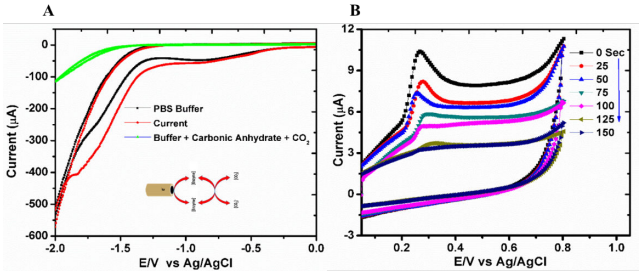

Figure 6: Cyclic voltammetry experiments for reduction of CAII with the preactivated CO_2 carboxylate molecule. Conditions: 10 ml of 0.1 M PBS (pH 5); 0.2% (v/v) CAII and CO_2 bubbled 5 min. Measuring conditions: voltage step of 0.006 V, scan rate of 100 mV s^{-1} at selected potential range.

Discussion

The hydration of CO_2 is the rate limiting step in current industrial carbon capture methods. Carbonic anhydrases have been used as biological catalysts for rapid hydration/ dehydration of industrial CO_2. Human CAII offers several advantages over other isoforms of CA as it shows a very high catalytic activity for the conversion of CO_2 to HCO_3^- and proton. CAII is an extremely efficient and specific means for CO_2 capture. However, current utilization of CAII in carbon capture is limited by the relative instability of the enzyme in high temperature. Hence, there is a need to improve upon the stability of CAII for the use in an industrial carbon sequestration. To achieve these aims, a prerequisite is to prepare the recombinant pure protein in high concentration. Bacterial expression system has been used to express CAII and purified from it. MD simulations were performed at different temperatures to check its stability. *In vitro* studies carried out to establish a correlation between *in vitro* and MD simulations results.

MD simulations

After simulating the CAII and CO_2 complex at different temperature each for 50 ns, their trajectories were analyzed by using the utilities of the GROMACS. The average distance between the CAII and CO_2 was calculated by using "gmx distance" utility of GROMACS.

In all studied conditions the distance between the two entities of the complex were remain relatively similar (Figure 1), which was observed in the range of 0.2 nm-0.3 nm. Furthermore, the RMSD values of the Cα atoms showed a varied nature. At 300K, the RMSD values were fluctuating around 0.3 nm up to 40 ns and the after that the magnitude of the values decreases (Figure 2A). The CAII showed similar fluctuating behavior at 310 K and 325 K with the RMSD values increases after 35 ns (Figure 2A). Moreover, the Rg curves showed similar behavior for 300 K and 310 K as the Rg values were obtained between 1.70 nm-1.75 nm, while relatively larger fluctuations were observed at 325 K, as the Rg values (<1.70 nm) were observed up to 25 ns and after that the Rg values may fluctuate beyond 1.75 nm (Figure 2B). Due to high temperature, the RMSF values showed higher fluctuation at 325 K as compared to the other conditions (Figure 2C). This indicates that the structural compactness of the CAII was maintained even at the higher temperatures and it can successfully detect the CO_2 even at the higher temperatures.

Expression and purification of CAII

CAII was successfully cloned and transformed into *E. coli* BL21 (DE3) strain for protein expression. CAII in *E. coli* BL21 (DE3) expressed and showing very high yield. SDS PAGE analysis showing that CAII found in the soluble bacterial extracts (supernanat). Furthermore, this supernatant was subjected to Ni-NTA affinity chromatography. The purified protein from Ni-NTA affinity showed contamination by other proteins (Figure 3A). The gel filtration chromatography was used to further purify the CAII. The purity of CAII was further confirmed by SDS-PAGE that clearly showing a single band (Figure 3C). Western blot and MALDI-TOF were also confirmed the CAII (Figure 3D).

Hydration of carbon dioxide with and without CAII

The rate limiting step in current industrial carbon capture methods is the hydration of CO_2. Figure 4 shows the curves show that this enzyme was a very effective catalyst for hydration of CO_2. CA catalyzes the hydration of CO_2 at high temperature (325 K) but below its melting temperature and it is an extremely efficient and specific method.

Acceleration of carbonate formation by CA

CAII provides bicarbonate at a rapid rate through the catalytic hydration of CO_2 by lowering the activation energy. As shown in Table 2, the amounts of calcium carbonate precipitated after 15, 30, and 60 sec is significantly higher than the control without enzyme at 325 K. The bicarbonate ions exist in equilibrium with carbonate ions and in presence of calcium ions result in calcium carbonate precipitation under the precipitation conditions (pH 9.0–9.5). Thus, CA plays the important role in hydration reaction corresponding to calcium carbonate formation; hence in the presence of enzyme the higher amount of the $CaCO_3$ is obtained at high temperature.

Figure 5 shows the XRD spectra of calcium carbonate obtained from CA (partially purified) and standard $CaCO_3$. Calcium carbonate ($CaCO_3$) has three crystal phases (calcite, aragonite, and vaterite). The calcite phase is a thermodynamically most stable phase under the ambient conditions. The XRD patterns of precipitates show major peaks at 23.05 (012), 29.40 (104), 31.44 (006), 35.97 (110), 39.41 (113), 43.16 (202), 47.51 (018), 48.50 (116) that match with the Joint Committee on Powder Diffraction Standards (JCPDS) data (JCPDS card number 86-2334) observed for calcite. This confirms that enzymatically formed calcium carbonate is the calcite phase. Similar results have been reported by Favre et al. [29] and Sharma et al. [27]. WDXRF analysis shows presence of Ca as major element correlating well with XRD data. The TEM analysis showed nano particle of $CaCO_3$ was found with size from 60 to 150 nm in presence of enzyme while without enzyme the size was not irregular in shape as shown in Figures 5A and 5B. This shows enzyme can be used for converting CO_2 to nano sized $CaCO_3$ which have several industrial applications. These finding are in good agreement with Sondi and Matijevi [32]. Therefore, CA could be used not only to sequester CO_2 but also to produce a valuable product even at high temperature. These nano-particles could be used in other industrial processes such as paper, ink, paint, or coating production plants which make the sequestration process economically desirable, and even profitable.

Electrochemical measurements

With reference to voltammogram in Figure 6A, shows that as we bubble more and more CO_2 in solution, the intensity of the current signal at E1/2 of -1.15 V is proportionally becoming more prominent while the opposite is true in Figure 6B. The peak observed is not well defined and it is understandable as reduction of CO_2 is a difficult problem owing to the fact that CO_2 is a very stable molecule [33].

In Figure 6A, there is a significant shift of the reduction potential from the catalytic run for CO_2 reduction versus the high-current irreversible electrochemical response in the presence of CAII [34]. This observation is agreement with the report by Reche and co-workers although the medium of electrochemical measurement is not the same [35,36].

Furthermore, Figure 6B shows an irreversible reduction peak at 0.276 ± 0.03 V (vs. Ag/AgCl) that is probably due to the reduction of the quinolone ring present in the CAII protein. As we bubble more and more CO_2 the intensity of the current signal is lowered. Altogether these results confirm that the prepared CAII is suitable for detection of the CO_2 at high temperature. It has been reported that a quinolone ring is reduced in the presence of CO_2. As the carbonic solution in the voltammetric cell becomes saturated with CO_2, at the pH of 6.8 there is an intense voltammetric peak at 0.6 V (vs Ag/AgCl) which appears to increase in current response arising from the response of the formic acid oxidation.

$$CO_2\,(g) \rightarrow CO_2(ads) \rightarrow CO(g)+CO_3^{2-}(aq)$$

The formation of $CO_2^{-\bullet}{}_{(aq)}$ is followed by disproportionation of $CO_2^{-\bullet}{}_{(ads)}$ and $CO_{2(g)}$ to give CO and CO_3^{2-}. There is also a high possibility of protonation of the $CO_2^{-\bullet}$, and likewise there is reduction of $COOH^{\bullet}$ to formate. Overall, it is understandable that CO_2 can produce a variety of intermediate/products which includes carbonates, oxalate, formate because there is a high density of LUMO of CO_2 that is found mainly on the carbon atom. Thus, during the electrochemical measurement there is a pH shift towards acidic medium and ultimately hinders detection as the hydrogen evolved reaction becomes a major interference.

Conclusions

We have successfully cloned, over expressed and purified CAII in high yield for CO_2 sequestration and bio-mineralization studies at high temperature (325 K). The recombinant protein CAII was used for these studies over other isoforms of CA because it has highest CO_2

hydration activity and converts CO_2 to $CaCO_3$ very efficiently. The potential for acceleration of CO_2 capture impressively illustrate the importance of CAII. The present work showed the biomineralization process for CO_2 hydration into calcium carbonate at high temperature. Furthermore, the voltammetric studies confirmed that CAII can successfully detect CO_2 in solution through the electrocatalytic performance of glassy carbon electrode even at 325 K. These results are very encouraging for the future development in which the electrode can be turned into an ideal tool of a CAII based biosensor. Moreover, the MD simulations results have been validated by *In vitro* studies that the CAII can detect the CO_2 even at higher temperatures and can be used for the detection of the pollutant CO_2. The studies showed the stability of CAII under high temperature (325 K) and confirmed the potential role in CO_2 sequestration. This study may be valuable in future to design the biodegradable industrial catalyst based on CAII to enhance CO_2 capture rate and to diminish its environmental collision.

Acknowledgement

DI is thankful to Grants Commission (UGC), New Delhi, India, for providing DS Kothari fellowship. We sincerely thank Dr. Abdul Waheed, Saint Louis University, Saint Louis for providing CAII clone. The authors like to express their gratitude towards the Center for High Performance Computing (CHPC), Cape Town, South Africa for providing the computational infrastructure.

Author Disclosure Statement

The authors declare that no conflicting financial interests exist.

References

1. Keeling CD, Whorf TP, Wahlen M, Van der Plichtt J (1995) Interannual extremes in the rate of rise of atmospheric carbon dioxide since 1980. Nature 375: 666-670.
2. Raupach MR, Marland G, Ciais P, Le Quéré C, Canadell JG, et al. (2007) Global and regional drivers of accelerating CO_2 emissions. Proceedings of the National Academy of Sciences 104: 10288-10293.
3. McKibbin WJ, Wilcoxen PJ (2002) The Role of Economics in Climate Change Policy. Journal of Economic Perspectives 16: 107-29.
4. McNamara ND, Hicks JC (2014) CO_2 Capture and Conversion with a Multifunctional Polyethyleneimine-Tethered Iminophosphine Iridium Catalyst/Adsorbent. Chem Sus Chem 7: 1114-1124.
5. Gao WY, Chen Y, Niu Y, Williams K, Cash L, et al. (2014) Crystal engineering of an nbo topology metal-organic framework for chemical fixation of CO_2 under ambient conditions. Angew Chem Int Ed Engl 53: 2615-2619.
6. Kimura T, Kamata K, Mizuno N (2012) A bifunctional tungstate catalyst for chemical fixation of CO_2 at atmospheric pressure. Angewandte Chemie International Edition 51: 6700-6703.
7. Mirjafari P, Asghari K, Mahinpey N (2007) Investigating the application of enzyme carbonic anhydrase for CO_2 sequestration purposes. Industrial & Engineering Chemistry Research 46: 921-926.
8. Luca VD, Vullo D, Scozzafava A, Carginale V, Rossi M, et al. (2013) An alpha-carbonic anhydrase from the thermophilic bacterium Sulphurihydrogenibium azorense is the fastest enzyme known for the CO_2 hydration reaction. Bioorg Med Chem 21: 1465-1469.
9. Pinsent BRW, Pearson L, Roughton FJW (1956) The kinetics of combination of carbon dioxide with hydroxide ions. Transactions of the Faraday Society 52: 1512-1520.
10. Supuran CT (2008) Carbonic anhydrases-an overview. Current Pharmaceutical Design 14: 603-614.
11. Hassan MI, Shajee B, Waheed A, Ahmad F, Sly WS (2013) Structure, function and applications of carbonic anhydrase isozymes. Bioorganic & medicinal chemistry 21: 1570-1582.
12. Supuran CT, Scozzafava A, Casini A (2003) Carbonic anhydrase inhibitors. Med Res Rev 23: 146-189.
13. Bootorabi F, Janis J, Valjakka J, Isoniemi S, Vainiotalo P, et al. (2008) Modification of carbonic anhydrase II with acetaldehyde, the first metabolite of ethanol, leads to decreased enzyme activity. BMC Biochem 9: 32
14. Saville CaL JJ (2011) Biotechnology for the acceleration of carbon dioxide capture and sequestration. Curr Opin Biotech 22: 1-6.
15. Fulke AB, Mudliar SN, Yadav R, Shekh A, Srinivasan N, et al. (2010) Bio-mitigation of CO_2, calcite formation and simultaneous biodiesel precursors production using Chlorella sp. Bioresour Technol 101: 8473-8476.
16. Ramanan R, Kannan K, Deshkar A, Yadav R, Chakrabarti T (2010) Enhanced algal CO_2 sequestration through calcite deposition by Chlorella sp. and Spirulina platensis in a mini-raceway pond. Bioresour Technol 101: 2616-2622.
17. Lindskog S, Silverman DN (2000) he catalytic mechanism of mammalian carbonic anhydrases. In: Carbonic Anhydrases, pp: 175-195.
18. Liu Z, Bartlow P, Dilmore RM, Soong Y, Pan Z, et al. (2009) Production, purification, and characterization of a fusion protein of carbonic anhydrase from Neisseria gonorrhoeae and cellulose binding domain from Clostridium thermocellum. Biotechnol Prog 25: 68-74.
19. Kanbar B, Ozdemir E (2010) Thermal stability of carbonic anhydrase immobilized within polyurethane foam. Biotechnology Progress 26: 1474-1480.
20. Vanommeslaeghe K, Hatcher E, Acharya C, Kundu S, Zhong S, et al. (2010) CHARMM general force field: A force field for drug-like molecules compatible with the CHARMM all-atom additive biological force fields. J Comput Chem 31: 671-690.
21. Kim CU, Song H, Avvaru BS, Gruner SM, Park S, et al. (2016) Tracking solvent and protein movement during CO_2 release in carbonic anhydrase II crystals. Proceedings of the National Academy of Sciences 113: 5257-5262.
22. Pronk S, Pall S, Schulz R, Larsson P, Bjelkmar P, et al. (2013) GROMACS 4.5: a high-throughput and highly parallel open source molecular simulation toolkit. Bioinformatics 29: 845-854.
23. Oostenbrink C, Villa A, Mark AE, van Gunsteren WF (2004) A biomolecular force field based on the free enthalpy of hydration and solvation: the GROMOS force-field parameter sets 53A5 and 53A6. J Comput Chem 25: 1656-1676.
24. Schuttelkopf AW, van Aalten DM (2004) PRODRG: a tool for high-throughput crystallography of protein-ligand complexes. Acta Crystallogr D Biol Crystallogr 60: 1355-1363.
25. Frisch MJ, Trucks GW, Schlegel HB, Scuseria GE, Robb MA, et al. (2009) Gaussian 09. Wallingford, CT, USA: Gaussian.
26. Zielkiewicz J (2005) Structural properties of water: comparison of the SPC, SPCE, TIP4P, and TIP5P models of water. J Chem Phys 123: 104501.
27. Sharma A, Bhattacharya A, Shrivastava A (2011) Biomimetic CO_2 sequestration using purified carbonic anhydrase from indigenous bacterial strains immobilized on biopolymeric materials. Enzyme Microb Technol 48: 416-426.
28. Ho C, Sturtevant JM (1963) The Kinetics of the Hydration of Carbon Dioxide at 25 Degrees. J Biol Chem 238: 3499-3501.
29. Nathalie Favre MLC, Alain CP (2009) Biocatalytic capture of CO_2 with carbonic anhydrase and its transformation to solid carbonate. Journal of Molecular Catalysis B: Enzymatic 60: 163-170.
30. da Costa Ores J, Sala L, Cerveira GP, Kalil SJ (2012) Purification of carbonic anhydrase from bovine erythrocytes and its application in the enzymic capture of carbon dioxide. Chemosphere 88: 255-259.
31. Jo BH, Kim IG, Seo JH, Kang DG, Cha HJ (2013) Engineered Escherichia coli with periplasmic carbonic anhydrase as a biocatalyst for CO_2 sequestration. Appl Environ Microbiol 79: 6697-6705.

32. Sondi I, Matijevic E (2001) Homogeneous Precipitation of Calcium Carbonates by Enzyme Catalyzed Reaction. J Colloid Interface Sci 238: 208-214.
33. Pulidindi IN, Kimchi BB, Gedanken A (2014) Selective chemical reduction of carbon dioxide to formate using microwave irradiation. Journal of CO_2 Utilization 7: 19-22
34. Luca OR, McCrory CC, Dalleska NF, Koval CA (2015) The Selective Electrochemical Conversion of Preactivated CO_2 to Methane. Journal of The Electrochemical Society 162: 473-476.
35. Reche I, Gallardo I, Guirado G (2015) Cyclic voltammetry using silver as cathode material: a simple method for determining electro and chemical features and solubility values of CO_2 in ionic liquids. Physical Chemistry Chemical Physics 17: 2339-2343.
36. Reche I, Gallardo I, Guirado G (2014) Electrochemical studies of CO_2 in imidazolium ionic liquids using silver as a working electrode: a suitable approach for determining diffusion coefficients, solubility values, and electrocatalytic effects. RSC Advances 4: 65176-65183.